



**CHALMERS**  
UNIVERSITY OF TECHNOLOGY

# **Evaluating the anti-icing performance of Hydronic Heating system in pedestrian pavement**

Master's Thesis in Infrastructure and Environmental Engineering MPIEE

ABOBAKKAR NAKEEB ALI  
MOKSHITH YADAVA SALIAN

**DEPARTMENT OF ARCHITECTURE AND CIVIL ENGINEERING**

---

CHALMERS UNIVERSITY OF TECHNOLOGY

Gothenburg, Sweden 2024  
[www.chalmers.se](http://www.chalmers.se)

MASTER'S THESIS ACEX30

# Evaluating the anti-icing performance of Hydronic Heating system in pedestrian pavement

ABOBAKKAR NAKEEB ALI  
MOKSHITH YADAVA SALIAN



**CHALMERS**  
UNIVERSITY OF TECHNOLOGY

*Department of Architecture and Civil Engineering*

CHALMERS UNIVERSITY OF TECHNOLOGY  
Gothenburg Sweden 2024

# Evaluating the anti-icing performance of Hydronic Heating system in pedestrian pavement

ABOBAKKAR NAKEEB ALI  
MOKSHITH YADAVA SALIAN

© ABOBAKKAR NAKEEB ALI, MOKSHITH YADAVA SALIAN, 2024

Examiner and Supervisor: Pär Johansson, Chalmers University of Technology  
Industrial Supervisor: Raheb Mirzananadi, VTI

Master's thesis 2024: ACEX30  
Department of Architecture and Civil Engineering  
Chalmers University of Technology  
SE-41296 Gothenburg  
Sweden 2024  
Telephone: +46(0)31-772 1000

# Abstract

This thesis explores the performance and feasibility of using Hydronic Heating Pavement (HHP) systems for anti-icing and solar energy harvesting on pedestrian pathways and roadways. Two test sites were selected for analysis: the E18 motorway in Östersund and a pedestrian pathway in Gothenburg. The study employed numerical modeling using COMSOL Multiphysics 6.2 to simulate surface temperatures and assess energy requirements. Data including air temperature, dew point, wind speed, precipitation, and radiation were collected from local sources and used to validate the models. The numerical simulations demonstrated that, without heating, the road surface in Östersund experienced up to 2,121 hours of slippery conditions annually, whereas the installation of heating pipes reduced this to 332 hours in Gothenburg's pedestrian pathway. The annual energy required for anti-icing the pedestrian pathways was calculated to be 62.4 kWh/m<sup>2</sup>/year, with a mean heat flow of 481.3 W/m from a single pipe. Sensitivity analysis revealed that factors such as pipe distance, thermal conductivity, and fluid temperature significantly impacted system performance. For instance, increasing the pipe spacing doubled the number of slippery hours, while higher thermal conductivity and absorptivity reduced them. Comparisons between roads and pedestrian pathways showed that pedestrian pathways required significantly less energy (seven times lower) due to their narrower width. The results indicate that solar energy harvesting alone is more than sufficient to meet the system's energy requirements, providing up to five times the total annual energy needed when optimized during the summer months. This study concludes that the hydronic heating pavement system demonstrates significant potential in enhancing safety and minimizing icy conditions on pedestrian pathways. Furthermore, the renewable solar energy harvested is capable of fully supporting the operation of HHP system without any additional inputs.

# Acknowledgement

This thesis would not have been possible without the exceptional collaboration and support from Chalmers University of Technology, The Swedish National Road and Transport Research Institute (VTI), Swedish Meteorological and Hydrological Institute (SMHI) and Trafikverket for their Support and guidance throughout this work.

We would like to extend our sincere gratitude to our supervisor and examiner Pär Johansson for their motivation and support for the success of this work.

Above all, we would like to extend our sincere gratitude to our supervisor Raheb Mirzanimadi from VTI, For their ongoing support, motivation, and expert advice throughout the research process. Their insights and expertise were crucial at every stage of this research.

We would like to express our special gratitude to Susanne Tainamo from SMHI and Mats Riehm from Trafikverket For their cooperation and openness in providing important data and insights. which were a very important part of the success of this work. Your input has been priceless, and we greatly appreciate your effort

Finally, we would like to extend our special gratitude to our family and friends, your constant support and belief in us has consistently inspired and motivated us

## Table of Contents

1. Introduction .....	5
1.1 Background .....	5
1.2 Gap identification .....	6
1.3 Aim and research question .....	7
1.4 Limitations .....	7
2. Literature review.....	8
3. Theory .....	10
3.1 heat balance theory .....	10
3.2 Equivalent heat equations.....	12
4. Methodology .....	14
4.1 Data collection .....	14
4.1.1 Gothenburg site .....	14
4.1.2 Test site E18 .....	16
4.1.3 Properties of asphalt materials. ....	19
4.2 Numerical model of HHP systems .....	19
5. Results .....	22
5.1 Validation of test site E18 .....	22
5.2 Numerical modelling of Gothenburg site .....	26
5.2.1 The required energy for anti-icing and slippery conditions of road surface.....	28
5.3 Sensitivity Analysis for different parameters .....	29
5.3.1 Thermal conductivity of wearing layer .....	29
5.3.2 Distance between the pipes.....	29
5.3.3 Fluid temperature.....	30
5.3.4 Absorptivity of the road surface .....	31
5.3.5 Embedded depth of pipe .....	31
6. Summary and Conclusion.....	33
7. Future work .....	35
Reference .....	36
Appendix .....	39

# 1. Introduction

This study focuses on the main problems caused by snow and black ice on roads in Gothenburg during winter. Since most people in Gothenburg rely on public transportation, it becomes difficult for commuters when services are disrupted by snow. Often transportation halts due to ice on the roads, forcing people to walk long distances to reach their destination. While walking, people often use pedestrian paths, even though snow is usually cleared only from main roads. Since there is less attention on clearing snow from pedestrian paths, people are more likely to slip and fall, leading to accidents and more dangerous situations. To address this issue, a small study was conducted to explore potential solutions. Multiple research papers were reviewed, and various methods to tackle snow were analyzed, but no better or sustainable solution was found. This is when the concept of Hydronic Heating Pavement system (HHP) was discovered from (Mirzanimadi, Hagentoft, Johansson, et al., 2018). Hydronic Heating Pavement systems were a detailed solution implemented on one of the roads in Sweden, but the challenge was how to apply the same solution to pedestrian paths. The focus was on determining how much energy could be saved and how effective it would be for the people commuting in snowy conditions.

Building on this, the study evaluates the HHP system for pedestrian paths, with a primary focus on the results from the E18 test site in Östersund. Additionally, a comparison study was conducted for Gothenburg using COMSOL Multiphysics 6.2 to assess maximum energy that could be saved on pedestrian paths compared to main roads. The model was developed for both pedestrian and main roads, validated using data from the E18 test site. The surface temperature was validated using a 1D numerical model. A 2D model was simulated to analyze annual energy required for anti-icing the road surface. Additionally, the mean heat required to pump through a single pipe for heat flow was calculated. The study also focuses on maintaining surface temperature to prevent slippery conditions and analyze the number of hours the road remains free from slipperiness.

## 1.1 Background

Ice and snow are the two beautiful elements that enhance the natural scenery in winter, but they also pose significant challenges to transportation. In addition to affecting roads, ice and snow has posed significant hazards to pedestrian pavement (Juga & Vajda, 2012). A hazard which was widely neglected is weather induced slippery sidewalk conditions leading to pedestrian slipping injuries and accidents (Hippi et al., 2020). While urban planning is the main aspect of developing a city or country, pedestrian behavior is quite essential (Liang et al., 2020). Cycling and walking is environmentally friendly having to be flexible, inexpensive, space efficiency and increase public health (Bärwolff et al., 2021a). but many academic institutions and social organizations such as the world health organization, The American planning association, the royal planning institute,

and the environmental protection agency from Sweden have raised huge concern over soft mobility as physical inactivity to be the 4th leading risk factor for global mortality (Liang et al., 2020a).

The research prioritizes pedestrian walkways due to significant emphasis placed on severe road accidents, often led to the frequent overlooking of pedestrian accidents and injuries. The Swedish transport administration has a long-term goal named Vision-Zero to completely avoid any death caused by traffic accidents, along with fatality rate due to seriously injured be reduced by 25% in the same time frame (Andersson, 2010). Road's experience frequent traffic movement generating a rolling action of friction that helps in snow melting but pedestrian walkways lack friction movement resulting in much slower snow melting (Hossain et al., 2014a). Two-thirds of pedestrians and cyclists fall under icy and snowy roads. In Sweden, 70% of bicycle accidents involve only one vehicle, with 40% of the accidents resulting from slippery roads. Approximately 51% of cycling accidents happen due to uncleared sidewalks or icy surfaces (Bärwolff et al., 2021a). In Sweden snow and ice contributes from 40-80% of single pedestrian accidents, 36% of the reported traffic accidents occurred between 2014-2019 were accounted for single pedestrian accidents with 24% resulted in serious injury (Eriksson et al., n.d.).

To tackle the issue of ice and snow there are numerous ways, but the most practical and most installed systems are plowing, chemical usage, abrasive and snow melting by thermal systems (Xu et al., 2018). Plowing snow is the most common method of removing snow and ice, with low moisture content and temperature far from melting point snow can be easily plowed from road surface (Michelle Akin et al., 2013). While high efficiency melting techniques are still being developed, these techniques have produced good results for the past 60 years (Yu et al., 2014).

## 1.2 Gap identification

Despite the advancements in the use of Hydronic Heated Pavement system for main roads, there is a gap in the application of HHP system for pedestrian paths, particularly in terms of energy efficiency and optimization. The main difference in the structure of main roads and pedestrian paths is their width, pavement structure and the load applied on the road. The load is the key factor that differentiates the pavements, along with the differences in thickness, bearing capacity and material properties.

For main roads, the aim of anti-icing is to eliminate ice across the full width of the road. However, for pedestrian paths, it is possible to eliminate ice across only a narrower part of the width, which could result in lower energy requirements. The gap exists in understanding how to effectively apply HHP for anti-icing on pedestrian pathways, considering the reduced width and load.

This study aims to utilize HHP on pedestrian pathways for harvesting solar energy, considering the entire width of the pathway but applying anti-icing to only a narrow section. This could lead to energy savings, improving efficiency in keeping pedestrian paths safe during snow and ice conditions.

## 1.3 Aim and research question

To investigate the feasibility of utilising the HHP system for collecting solar energy and anti-icing measures on pedestrian roads. To analyse how various design options of Hydronic Heating Pavement systems impact the anti-icing performance using a numerical simulation model.

Few research questions in this thesis are:

1. The performance of the HHP system on pavement pathways and the comparison of its performance on roads.
2. Sensitive analysis of different parameters of the HHP system and pavement properties on the feasibility of HHP.
3. What is the potential of using renewable energy (here solar energy) to implement HHP?

## 1.4 Limitations

There is uncertainty between the measured surface temperature and the calculated surface temperature. The primary factors contributing to these uncertainties are global radiation, wind speed, and sky temperature. Wind speed data was available at a height of 10 meters, but the value was adjusted for a height of 1 meter for accuracy. Sky temperature was calculated using a different equation, so there is uncertainty in the sky temperature and data for global radiation was not available from the same location, hence values were collected from a nearby station. These factors are the main contributors to the uncertainties. However, efforts were made to minimize these uncertainties as much as possible.

Due to the significant variation in air temperature between summer and winter, the average air temperature was taken as the initial temperature in the COMSOL model.

## 2. Literature review

This section presents the literature review for the thesis timeline, beginning with the winter and snow season, where ice accumulates on the ground. This accumulation causes various problems, including safety risks and operational inefficiencies. The review discusses different approaches used to tackle these issues, comparing their effectiveness. Based on the analysis, a potential solution was selected, which offers a more effective way of dealing ice-related challenges.

To tackle the ice and snow problems, (Liang et al., 2020b) used computer vision technology to analyse video footage and study how weather effect the walking speed and he concluded that winter conditions including temperature and ground conditions impact the pedestrian speed. (Fossum & Ryeng, 2022) conducted observational studies and surveys to investigate pedestrian behaviour and route choice in the different winter condition to conclude that Surface condition effect the walking speed and pedestrians change their route while walking pattern and also gritted ice reduces the risk of accident. (Bärwolff et al., 2021b) conducted Video recording and pedestrian surveys in icy condition and comparing with other seasons data and found out that the snow and ice cause most pedestrians and cyclists falls in winter, and poorly maintained road increase the risk, he concluded by mentioning that maintained road with de-icing sanding will prevent falls.

(Gitelman et al., 2012) studied different international comparisons, detailed analysis of national statistics, and the development of an accident typology at Israel and concluded that Pedestrian fatalities in Israel are higher than most EU countries, most pedestrian fatalities in Israel happen on urban roads crossing and ten main patterns of pedestrian accidents were identified in Israel. (Levulyte, 2017) studied the analysis of pedestrian accident and analysis of crossing design and concluded that used smart system (Sensors) in the vehicle to detect the pedestrian movement and using the real time communication between vehicle and pedestrians. (Narváez et al., 2019)'s study observed risky pedestrian behaviours at busy intersections, made a survey and analysed answers from 1536 peoples using simple statistical correlations and concluded that in the analysis it is found that young people use phone and old people skip crosswalk while crossing the road, leading to 18.5% of people involved in an accident. Therefore, education of road safety is also important with infrastructure.

According to (Glagolev et al., 2018) Testing and comparing anti-icing materials for road safety shows that the new generation anti-icing material improve the road cohesion by 24% and reduce the braking distance by 25% to improve the road safety. (Hossain et al., 2014b) Experiments with different types of salt and different road condition (ploughed and not ploughed) to check the anti-icing and de-icing effectiveness to conclude that the anti-icing treatment is most effective before light snow and with brine and solid salt, but less effective during heavy snow. (Yu et al., 2014) tested the two methods used to deal with snow clearance and melting. The clearance involves manually removing snow using machines and melting involves using chemical melting, thermal

melting while using sand and salts and concluded that Snow-melting agents like chemicals or salts are very expensive and harmful to the environment, so mechanized snow removal techniques and de-icing machines should advance further and be used instead of chemicals and salts.

Hydronic snow melting system is a closed loop tube made with flexible polymer (e.g., cross-linked polyethylene, or PEX) which circulate the warm fluid like glycol and hot water mix. The pipe made up with the PEX material embedded inside the Structure of the asphalt road. The fluid is warmed to the temperature between 140°F to 180°F to flow inside the pipe and which produces heat to the surface, which melts the snow in the surface. The cold-water mixture flows to the energy source and the cycle repeats. The pollution caused by HHP to the environment is very less compared to the other snow melting process. (Mirzanimadi, 2017).

The main factors like a) Distance between the pipe(mm), b) Embedded depth of the pipe(mm), c) Fluid temperature inside the pipe (°C), d) Absorptivity on the road surface and e) Thermal conductivity (W/m. K) of the asphalt layer will affect the performance of the HHP.

# 3. Theory

This section represents all the important factors that are to be considered in the heat transfer to design the hydronic heating systems in pedestrian pavements, (Mirzanamadi, Hagentoft, Johansson, et al., 2018; Mirzanamadi, 2019). and different models used to calculate the sky temperature.

## 3.1 heat balance theory

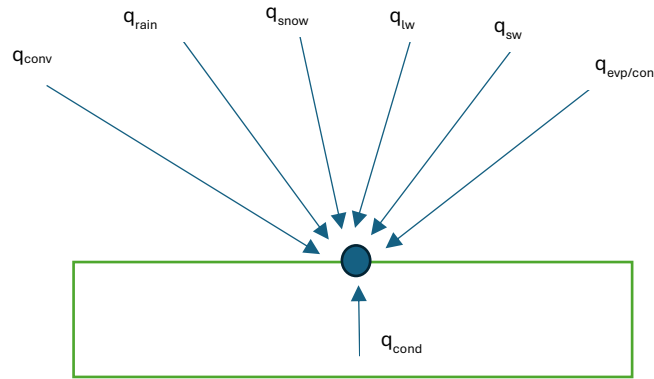


Figure 1: Heat balance of the road surface. (Mirzanamadi, 2017)

Figure 1 represents a heat balance for the pavement surface. For the analysis of pedestrian pavements several assumptions are simplified, it is assumed that the snow is removed from the pavement, so the energy supply is not used to melt snow. The road condition is assumed to be non-slippery for pedestrians, thus heat generated from sources like nearby traffic or buildings is excluded. An effective drainage system is in use, to the flow of existing snow and rainwater are drained from the pavement surface. The pavement heating system is to prevent slippery conditions caused by condensation and freezing. When the temperature of the surface gets below 0° C and condensation occurs, ice forms.

This section visualizes the mass and heat balance of condensation and evaporation for pavement surfaces. For the heat balance of roads, several heat factors are considered, they are.

$$q_{conv} + q_{cond} + q_{rain} + q_{snow} + q_{lw} + q_{sw} + q_{evp/con} = 0 \tag{1}$$

Where Convective heat transfer ( $q_{conv}$ )W/m is the exchange of heat between surface and ambient air (heat due to air movement across the surface).

$$q_{conv} = h_c \cdot (T_{ambient} - T_{surface}) \tag{2}$$

Where  $T_{ambient}$  is the ambient temperature,  $T_{surface}$  is the surface temperature and  $h_c$  (W/ m<sup>2</sup> K) is the convective heat transfer co-efficient.

$$h_c = 6 + 4 \times v \quad (v \leq 5 \text{ m/s}) \quad (3)$$

$$h_c = 7.41 \times v^{0.78} \quad (v > 5 \text{ m/s}) \quad (4)$$

Where  $v$  (m/s) is the wind speed.

To calculate the convective heat transfer coefficient ( $h_c$ ), the wind speed value should be as close to the road level as possible. Wind speed data was obtained at a height of 10 meters, but for accuracy, it was necessary to adjust this value to 1 meter. The following equation from (Mirzanamadi, 2017) was used for this adjustment.

$$v_z = v_m \cdot k \cdot z^a \quad (5)$$

Where  $v_z$  (m/s) is the value of wind speed at the height of  $z$  meter,  $v_m$  (m/s) is the wind speed at 10-meter height,  $k = 0.68$  and  $a = 0.17$  are the constant parameters for an open and flat area from Hagentoft 2001.

Conductive heat flux ( $q_{cond}$ ) W/m is the heat conducted from ground or any embedded heating pipes to surface, including artificial heating systems installed to keep surface warm.

$$q_{cond} = - \lambda \cdot \nabla T \quad (6)$$

Where  $\lambda$  (W/ m K) is the thermal conductivity of road materials,  $T$  (K) is the temperature and thermal conductivity of concrete,  $\lambda_{concrete} = 1.6$  W/m K.

Sensible heat from rain ( $q_{rain}$ ) W/m is the heat from rainwater falling on surface (depending on surface temperature, rain can add or remove heat from surface.

$$q_{rain} = m_{rain} \cdot C_{p-water} \cdot (T_{ambient} - T_{surface}) \quad (7)$$

Where  $m_{rain}$  is the Rainfall rate per m<sup>2</sup> and  $C_{p-water}$  is the Heat capacity of water [4181 J/Kg K].

Sensible heat from snow ( $q_{snow}$ ) W/m is like rain; snow can affect surface temperature based on the phase change involved when snow melts.

$$q_{snow} = m_{snow} \cdot C_{p-snow} \cdot (T_{ambient} - T_{surface}) \quad (8)$$

Where  $m_{snow}$  is the Snowfall rate per m<sup>2</sup>,  $C_{p-snow}$  is the Heat capacity of ice crystals in snow and [ $C_{p-snow} = 2100$ J/Kg.K].

Long wave radiation ( $q_{lw}$ ) W/m is the loss or gain of heat due to infrared radiation emitted by surface and absorbed from surroundings. These can also absorb radiation from nearby objects and the sky.

$$q_{lw} = \varepsilon \cdot \sigma \cdot (T_{sky}^4 - T_{surface}^4) \quad (9)$$

Where  $\varepsilon$  is the Emissivity of surface [0.81-0.98],  $\sigma$  is the Stefan Boltzmann constant [ $5.68 \times 10^{-8} \text{W/m}^2 \text{K}^4$ ],  $T_{sky} = \sqrt[4]{(q_{lw-incom}/\sigma)}$  and  $q_{lw-incom}$  is the Incoming long wave radiation.

Short wave radiation ( $q_{sw}$ )W/m is the heat or energy produced by sunlight, basically solar radiation.

$$q_{sw} = \alpha \cdot I \quad (10)$$

Where  $\alpha$  is the solar absorptivity of surface and  $I$  is the solar irradiation ( $\text{W/m}^2$ ).  $\alpha$  depends on the color, wherein  $\alpha$  is 0.96 for black asphalt pavement and 0.6 for white asphalt pavement.

Latent heat of evaporation and condensation ( $q_{evp/cond}$ )W/m is the phase change of liquid on surface, condensation releases heat warming the surface and evaporation absorbs heat cooling the surface.

$$q_{evp/cond} = h_e \cdot \beta (V_{ambient} - V_s) \quad (11)$$

Where  $h_e$  is the latent heat of evaporation of water ( $2.5 \times 10^6 \text{ J/kg}$ ),  $V_{ambient}$  is the humidity by volume of ambient air,  $V_s$  is the humidity by volume of saturated air at surface temperature ( $\text{kg/m}^3$ ) and Lewis's formula  $\beta$  is the moisture transfer coefficient (m/s).

$$\text{Lewis's formula } \beta = \frac{h_c}{v_a c_{pa}} \quad (12)$$

Where  $h_c$  is the convective heat transfers co-efficient (10 to 100  $\text{W/m}^2\text{K}$ ) and  $P_a C_{pa}$  is the volumetric heat capacity of the ambient air atmospheric pressure ( $\text{J/m}^3\text{K}$ ).

## 3.2 Equivalent heat equations

Based on (Mirzanamadi et al., 2020; Mirzanamadi, Hagentoft, & Johansson, 2018). A simplified equation for heat balance is,

$$h_{eq} = h_c + h_r \quad (13)$$

$$T_{eq} = \frac{h_c \cdot T_{ambient} + h_r \cdot T_{sky} + \alpha \cdot I}{h_{eq}} \quad (14)$$

Where  $\alpha$  is the solar absorptivity of surface and  $\alpha$  depends on the color wherein  $\alpha$  is 0.96 for black asphalt pavement and 0.6 for white asphalt pavement.

(for the calculation of  $T_{eq}$ , the assumed value for absorptivity  $\alpha = 0.6$ ).

Where  $h_{eq}$  (W/ m<sup>2</sup> K) is equivalent heat transfer co-efficient and  $T_{eq}$  (K) is equivalent temperature.

$$h_r = \varepsilon \cdot \sigma \cdot (T_{sky}^2 + T_{ambient}^2) \cdot (T_{sky} + T_{ambient}) \quad (15)$$

Where,  $\varepsilon$  is the Emissivity of the road surface [0.81-0.98] and  $\sigma$  is the Stefan Boltzmann constant [5.68×10<sup>-8</sup>W/m<sup>2</sup> K<sup>4</sup>]

Further there are some models used to calculate the sky temperature. For numerical modelling of any pavement surface, several models have been developed to calculate the sky temperature. Based on the available long-wave radiation data, the sky temperature could have been calculated using the Theodore model from (Mirzanimadi, 2017). However, since the required long-wave and short-wave radiation data is unavailable for the selected area Gothenburg, an alternative model will be used to determine the value of  $T_{sky}$ .

Based on the models in the Table 1 , various  $T_{sky}$  models were calculated and the Hall et. al. equation was ultimately selected as it provided the most accurate results. These models were tested and analyzed under both summer and winter conditions over a span of three different years. The corresponding plots of the results are included in the appendix for reference

Table 1: reference models used to calculate the sky temperature based on (Mirzanimadi, 2017)

Reference	Equation
Hagentoft 2001	$T_{sky} = 1.2 * T_{Ambient} - 14$ (Clear sky) (16)
	$T_{sky} = T_{ambient}$ (Cloudy sky) (17)
Hall et al.2012k	$T_{sky} = T_{ambient} * (0.8 + \frac{T_{dew}-273.15}{250})^{0.25}$ (18)
Ramsey et al.1999	$T_{sky} = T_{ambient} - (1.1058 \cdot 10^3 - 7.562 * T_{ambient} + 1,333 \cdot 10^{-2} * T_{air}^2 - 31.292 * RH + 14.58 * RH^2)$ $T_{sky} = T_{ambient}$ (Cloudy sky)
Ramsey et al.1982	$T_{sky}=5.53 \cdot 10^{-2} * (T_{ambient})^{1.5}$
Denby et al.2013 (nortrip model)	$T_{sky}=T_{ambient} (0.23 + 0.443 * (\frac{p}{T_{ambient}})^{0.125})^{0.25}$ (Clear sky)
	$T_{sky}=0.99 * T_{ambient}$ $p=RH * 6.112 * \exp(\frac{17.76 * (T_{ambient}-273.15)}{T_{ambient}-29.65})$ (Cloudy sky)

# 4. Methodology

This section outlines the methods used for data collection from two different locations, Gothenburg and Test site E18. It also details the asphalt materials used at these sites and the numerical modeling approach applied to the Hydronic heating pavement system.

## 4.1 Data collection

To simulate the model, a comparison was needed to analyse the energy required for two different test sites. The E18 test site was chosen as a validation model and was simulated to determine the surface temperature. This was done to validate the test site and compare the results with the Gothenburg site, which was numerically simulated to calculate energy usage and assess the number of hours as slippery conditions on pedestrian paths.

### 4.1.1 Gothenburg site

The climate data are obtained from SMHI. A detailed data collection has been shown in Table 2

Table 2: overview of Data obtained from SMHI. (SMHI. , n.d.)

Parameters	Stations	Station no	Latitude	Longitude	Measuring height(m)
Air temperature	Göteborg A	71420	57.7156	11.9924	2
Precipitation	Göteborg A	71420	57.7156	11.9924	2
Relative humidity	Göteborg A	71420	57.7156	11.9924	2
Wind speed	Göteborg A	71420	57.7156	11.9924	10
Dew point temperature	Göteborg A	71420	57.7156	11.9924	2
Short wave radiation	Göteborg Sol	71415	57.6876	11.9796	2
Long wave radiation	Göteborg Sol	71415	56.6879	11.9796	2

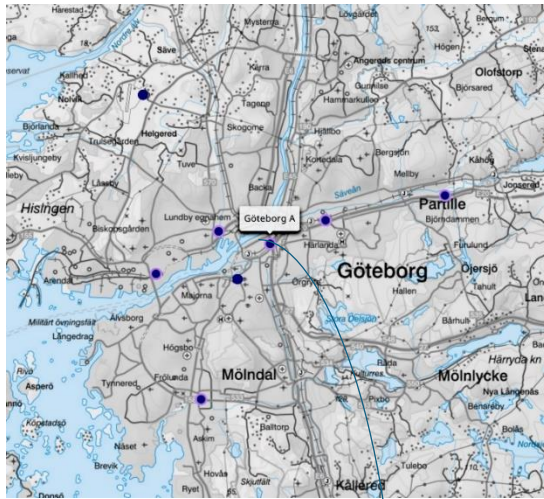


Figure 2: Location of Göteborg A

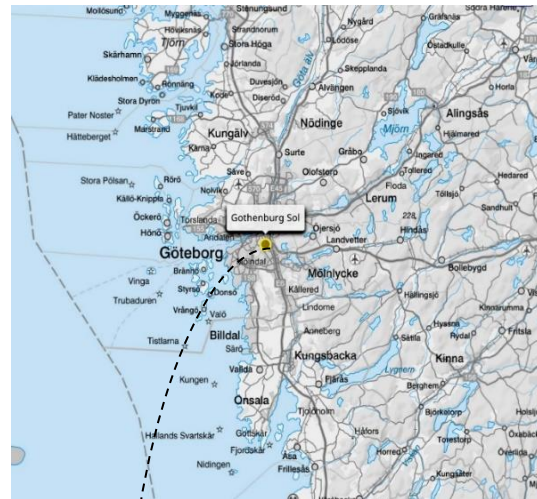


Figure 4: Location of Göteborg Sol



Figure 3: Location of Göteborg site

In order to collect data from Gothenburg site, initially multiple sources were referred and affirmed on collecting the data from the site SMHI. The test site was selected in common as Göteborg A, having data such as relative humidity (%), air temperature ( $^{\circ}\text{C}$ ), wind speed (m/s), precipitation (mm), dew point temperature ( $^{\circ}\text{C}$ ). Unfortunately for long wave radiation and short-wave radiation the test site had data missing for Göteborg A, where in Göteborg Sol was improvised. The data were for 3 years 2021, 2022 and 2023 in hourly interval.

The geographical boundary of the study is Västra götaland, particularly Göteborg the city in Sweden. Data such as short-wave radiation and long wave radiation has been collected from different locations as these data were not available for Goteborg A. the temporal boundary of the study is for 3 years (2021, 2022, 2023).

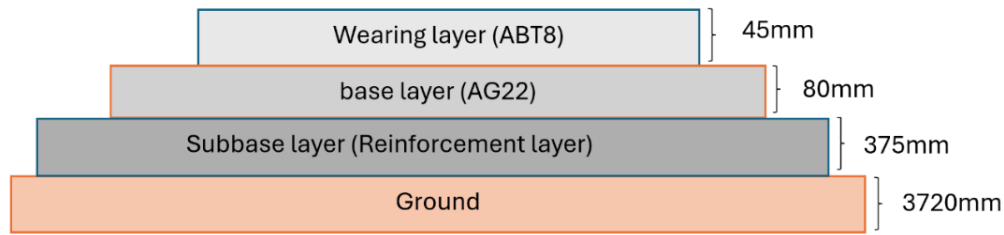


Figure 5: Pedestrian pavement profile for Gothenburg site. (Svelander & Turefeldt, n.d.)

According to (Svelander & Turefeldt, n.d.) the typical structure of a pedestrian road as shown in Figure 5 includes a wear-bearing layer made of ABT8, followed by a bearing layer composed of AG22. Beneath these, there is a reinforcement layer and the ground.

Since the pedestrian layer data was only available for Stockholm, it was assumed that the pedestrian pathway structure is generally similar between Stockholm and Gothenburg. Therefore, this structure was selected for the test site in Gothenburg. The Gothenburg site is a pedestrian pathway consisting of 4 layers designed for pedestrian traffic. The composition, thickness and the thermal properties of the layers were taken from Table 3.

Table 3: material properties corresponding to different road layers for Test site Gothenburg. (Svelander & Turefeldt, n.d.)

Reference	Material	Thickness (mm)	Thermal conductivity (w/ (m.K))	Density (kg/m <sup>3</sup> )	Specific heat capacity (J/ (kg. K))
(Svelander & Turefeldt, n.d.)	Wearing layer (ABT8)	45	2.24	2415	848
	Base layer (AG22)	80	0.7	1700	900
	Sub-base layer	375	0.8	1400	900
	Ground	3720	0.6	1300	600

#### 4.1.2 Test site E18

Several attempts were made to collect data from E18 test site, and eventually, a researcher from Trafikverket aided by sending emails and documents of the necessary data. Key information such as air temperature (°C), dew point temperature (°C), relative humidity (%), precipitation (mm) and wind speed (m/s) was obtained, along with surface temperature (°C). However, due to missing data for short-wave and long-wave radiation at E18 site, the data from the nearest station in Norrköping Sol was used from SMHI, assuming it would be similar to E18. The data collected was for the year 2023, in 10-minute intervals, which were later converted to hourly intervals.



Figure 6: Picture of the test site E18 obtained from (Sollén & Casselgren, 2021)

The E18 test site is a roadway consisting of six layers designed for vehicular traffic. The composition, thickness and the thermal properties of the layers were taken from Table 4.

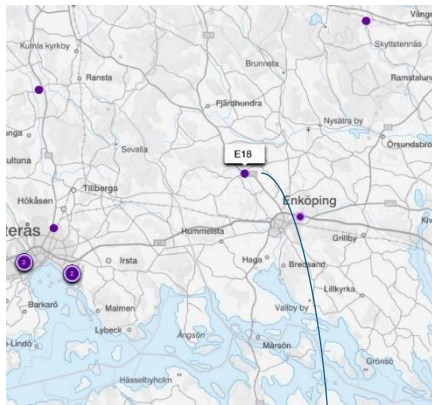


Figure 9: Location of E18 test site



Figure 8: Location of Norrköping Sol site

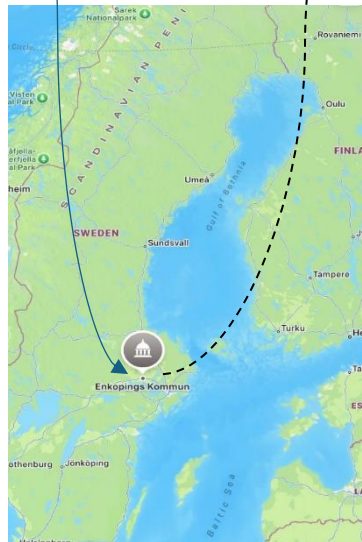


Figure 7: Location of E18 test site

The E18 test site was selected because existing results for the HHP systems are available from studies conducted there based on (Mirzanamadi, 2017). For the analysis, data were collected on air temperature(°C), relative humidity (%), dew-point temperature (°C), precipitation (mm), wind speed (m/s), short wave and long wave radiation (w/m<sup>2</sup>). The data was originally recorded at 10-minute intervals but was converted to hourly intervals for consistency. Since short-wave and long wave radiation data was unavailable for E18, it was collected from a nearby station in Norrköping.

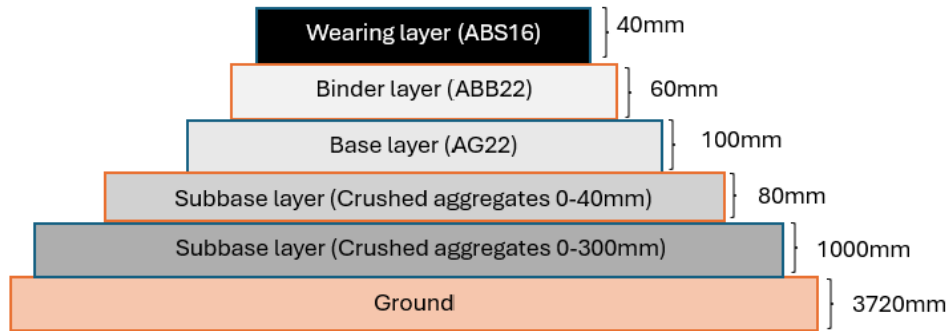


Figure 10: Road section profile of test site motorway E18. (Mirzanamadi, 2017)

In Sweden the first layer of asphalt (wearing layer) commonly uses material such as ABT11, ABS11 and ABS16. For the second layer (Binder layer) ABb22 is typically applied, while AG22 is used for the third layer (Base layer) (Mirzanamadi, 2017). A schematic diagram of the road layer is shown in Figure 10.

Table 4: material properties corresponding to different road layers for Test site

Reference	Material	Thickness( mm)	Thermal conductivity (W/ (m.K))	Density (kg/m <sup>3</sup> )	Specific heat capacity (J/ (kg. K))
(Mirzanamadi, 2017.)	Wearing layer (ABS16)	40	2.24	2415	848
	Binder layer (ABB22)	60	1.44	2577	822
	Base layer (AG22)	100	1.51	2582	894
	Subgrade layer	80	0.7	1700	900
	Subgrade layer	1000	0.8	1400	900
	Ground	3720	0.6	1300	600

### 4.1.3 Properties of asphalt materials.

There are several different types of asphalt materials used for roads in Sweden, the Table 5 based on (Mirzanimadi, Johansson, et al., 2018) represents the key properties of these materials, including the bitumen content (%), the air content (%), the density ( $\text{kg/m}^3$ ), aggregate sizes (mm) and the thermal conductivity ( $\text{W/m.K}$ ) providing a detailed comparison of their characteristics for various applications.

Table 5: Properties of asphalt materials for different asphalt layers. (Mirzanimadi, 2017)

ABT11	ABS11	ABS16	ABB22	AG22
Bitumen content:5.8%	Bitumen content:6.6 %	Bitumen content:6.4%	Bitumen content:4.9 %	Bitumen content:4.1 %
Air content: 2.1%	Air content: 2.8%	Air content: 1.7%	Air content: 3.6 %	Air content: 4.9 %
Density: 2,617kg/m <sup>3</sup>	Density: 2,421kg/m <sup>3</sup>	Density: 2,415 kg/m <sup>3</sup>	Density: 2,577 kg/m <sup>3</sup>	Density: 2,582 kg/m <sup>3</sup>
All aggregates are Diabase	Aggregates >4mm are quartzite, Aggregates<4mm are Diabase	Aggregates >4mm are quartzite, Aggregates<4mm are Diabase	All aggregates are Diabase	All aggregates are Diabase
Thermal conductivity: 1.39W/ (m.K)	Thermal conductivity: 1.89W/ (m.K)	Thermal conductivity: 1.51W/ (m.K)	Thermal conductivity: 2.24W/ (m.K)	Thermal conductivity: 1.44W/ (m.K)

The type of asphalt used in Sweden varies between pedestrian roads and main roads. Generally, the different types of asphalt layers include a) Dense asphalt concrete (ABT), b) Stone rich asphalt concrete (ABS), c) Asphalt gravel (AG), d) Asphalt binder base (ABb)

## 4.2 Numerical model of HHP systems

The numerical modeling of the HHP system was conducted to investigate its anti-icing operation. The focus of the study is on the numerical modeling of the HHP system for pedestrian pathways, while also validating results from main roads. Two different test sites were selected: E18 in Östersund and Gothenburg. Östersund experiences colder temperatures with less traffic, whereas Gothenburg has more varied weather conditions and heavier traffic. While Gothenburg doesn't experience prolonged cold like Östersund, it does have freezing periods.

Data for Gothenburg and E18 was collected from SMHI and Trafikverket. The dataset for Gothenburg was available in hourly intervals, while data for E18 was initially in 10-minute

intervals but was adjusted to hourly intervals for consistency in the analysis. The data collected included air temperature ( $^{\circ}\text{C}$ ), dew point temperature ( $^{\circ}\text{C}$ ), precipitation (mm), relative humidity (%), wind speed(m/s), long-wave radiation ( $\text{w}/\text{m}^2$ ) and short-wave radiation ( $\text{w}/\text{m}^2$ ). The numerical model was implemented using the implicit time-stepping method in COMSOL Multiphysics 6.2.

The 1D model was implemented in COMSOL for the E18 test site. The test site consisted of road layers based on the Östersund roadway, with specific thicknesses suitable for motorways. During the simulation, various Tsky models were tested to calculate the sky temperature, with the Hagentoft and Hall equations (16), (17) and (18) being the primary options. Ultimately, the Hall equation was selected, as it provided better surface temperature results in the simulation. Using this approach, the surface temperature was determined, and the number of hours with slippery conditions without the inclusion of heating pipes was measured.

The 2D model followed a similar process to the 1D model. Two different Tsky values were simulated, and once again, the Hall equation was chosen after validating the surface temperature. This model was then used for the 2D simulation.

Two different road layers with the property of a) Asphalt material, b) Thickness of each layer of road(mm), c) Thermal conductivity ( $\text{W}/(\text{m}\cdot\text{K})$ ), d) Density( $\text{kg}/\text{m}^3$ ) and e) Specific heat capacity ( $\text{J}/(\text{kg}\cdot\text{K})$ ) for test site E18 as well as Gothenburg were listed in Table 3 and Table 4.

A schematic layer of HHP system in the pedestrian pathway for the Gothenburg site is shown in Figure 11.

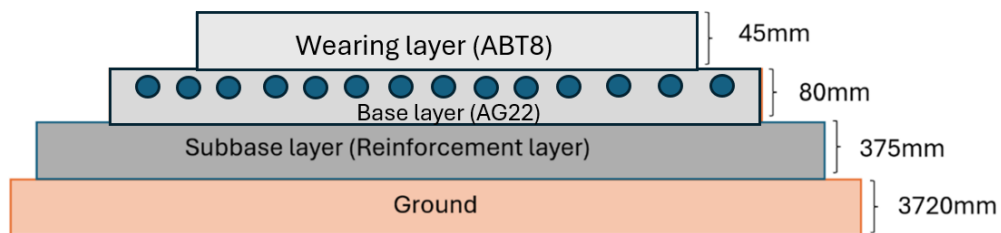


Figure 11: Scheme of the HHP system in a pedestrian pathway for Gothenburg site

The primary reason for focusing on pedestrian pathways is the increased walking time, accidents and stress during winter conditions. Pedestrian pathways often become the only mode of transportation when roads are blocked due to snow or ice. It can be assumed that the pipes in Gothenburg could be positioned higher, as there is less load falling on the pedestrian path compared to main traffic roads. The thermal properties of the road layers are as mentioned in Table

3, and a schematic pedestrian pathway with induced Hydronic heating pavement system is shown in Figure 11 contributing to reducing slippery conditions on the pedestrian pathways.

When the surface temperature falls below the dew-point temperature, moisture will form on the road surface. If the surface temperature is also lower than the freezing point of water, the moisture will turn into ice. Therefore, the HHP system must activate to heat the road and maintain the surface temperature above the dew-point temperature to prevent condensation. In doing so, even if the surface temperature remains below freezing, the road stays ice free (Mirzanimadi, 2017).

The Hydronic Heating Pavement system will run when the following conditions are satisfied,

$$\{T_{surface} < 0^{\circ} C \quad (19)$$

Here, the surface temperature is the temperature at the midpoint between the heating pipes. When heating is activated, the fluid circulating through the pipes is set to a temperature of 10 °C. Once the heating is stopped, the boundary condition at the inner surface of the pipe walls is set to be adiabatic. By calculating the heat flow from a single pipe, the annual energy required for anti-icing the road surface,  $E_r$  can be determined using the following formula,

$$E_r = \frac{W}{c} \cdot \int_{t=0}^{1\text{year}} q_{pipe-heating} \cdot dt \quad (20)$$

Where  $c$  (m) is the distance between the pipes and  $W$ (m) is the width of the road,  $W = 1\text{m}$ .

Further, the number of hours of the slippery condition on the road surface is calculated when the temperature of the road surface is lower than 0°C.

$$t_{slippery} = \int_0^{1\text{year}} f \cdot dt \quad (f = 1 \text{ if } (T_{surface} < 0^{\circ} C) \text{ otherwise } f = 0) \quad (21)$$

# 5. Results

The results are based on the validation of the test site E18, the numerical modelling of Gothenburg site, the annual energy required and the remaining number of hours with slippery conditions on the road surface when using the Hydronic Heating Pavement system including sensitivity analysis.

## 5.1 Validation of test site E18

Initially, the sky temperature was intended to be calculated using incoming long wave radiation. However, after analyzing six different  $T_{sky}$  models, the hall and Hagentoft models from equations (16), (17) and (18) were considered.

Hall Model:

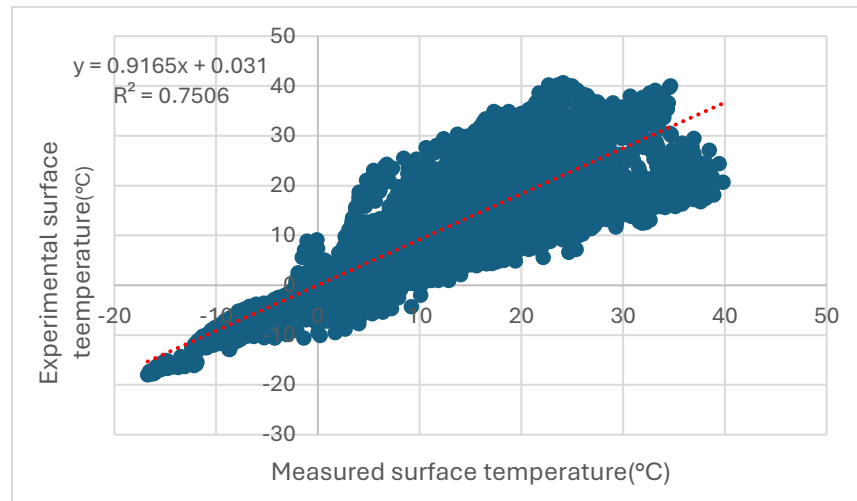


Figure 12: Scatter plot of comparing the surface temperature from the numerical and measured data using Hall equation

From the Figure 12, the Equation:  $y=0.9165x+0.031$  and  $R^2$  value: 0.7506, the obtained slope (0.9165) is close to 1, meaning the predictions of this model are quite similar to the actual data (a slope of 1 would mean a perfect match between predictions and actual values).  $R^2 = 0.7506$  indicates that 75.06% of the variation in the surface temperature is explained by the model. It's a reasonably good fit.

## Hagentoft Model:

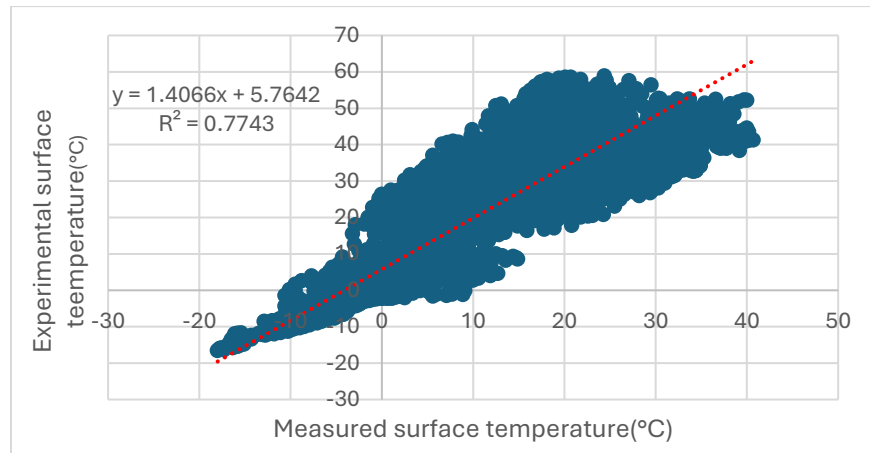


Figure 13: Scatter plot of comparing the surface temperature from the numerical and measured data using Hagentoft equation

From the Figure 13, the Equation:  $y=1.4066x+5.7642$  and  $R^2$  value: 0.7743, the obtained slope (1.4066) is farther from 1, indicating that this model tends to overpredict compared to the actual data (it predicts higher temperatures).  $R^2 = 0.7743$  means 77.43% of the variation is explained, so it fits the data slightly better than the Hall model, but not by a huge margin.

Based on the  $R^2$  values:

The Hagentoft model has a slightly better fit ( $R^2 = 0.7743$  vs. 0.7506), meaning it explains more of the variation in the data. However, the Hall model has a slope (0.9165) that is much closer to 1, meaning its predictions are closer to the actual values, while the Hagentoft model overpredicts (slope = 1.4066).

Hence the Hall model is chosen as its slope is closer to 1, having more accurate in predicting values closer to the actual surface temperature. Although its  $R^2$  value (0.7506) is slightly lower, it still has explanation for the variation in the data.

Based on the validation of Test site E18, Table 6 represents the mean temperature difference and the standard deviation of the road surface layer for the year 2023. The temperature difference is the difference in the measured data versus the numerical data. for the numerical modelling the absorptivity and emissivity were set to 0.6 and 0.9. The surface temperature comparison after the simulation in COMSOL is presented in Figure 14. This illustrates the graph for surface temperature versus the measured and numerically obtained surface temperature. The T. Diff. obtained is 1.62 and the S.D. of 2.28 for October of 2023.

Table 6: Mean surface temperature difference between measured and numerical model and its standard deviation for the year 2023.

Months	Mean temperature difference	Standard deviation
January	1.44	1.35
February	1.92	2.43
march	1.62	3.54
April	-0.64	5.85
may	-1.37	7.91
June	1.71	9.89
July	0.96	7.49
august	-0.23	5.43
September	0.66	4.62
October	1.62	2.28
November	0.77	1.29
December	0.97	1.3

The validation results showed that the annual mean temperature difference is 0.77°C between the surface temperature obtained from the numerical model and the measured data, with a standard deviation of 5.48°C

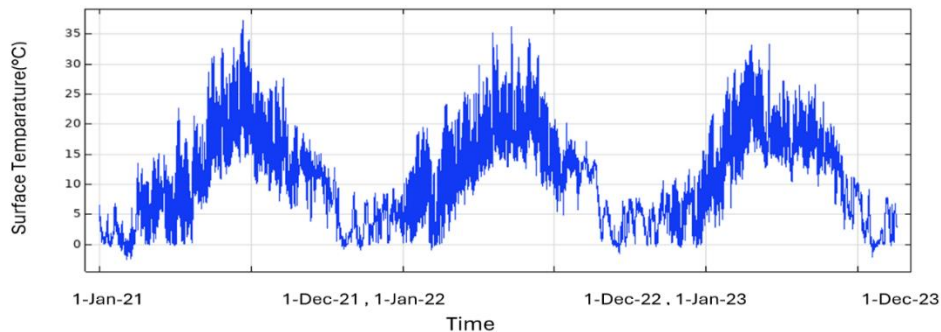


Figure 14: Numerical calculated surface temperature using the climate data of Gothenburg for the case without heating pipe

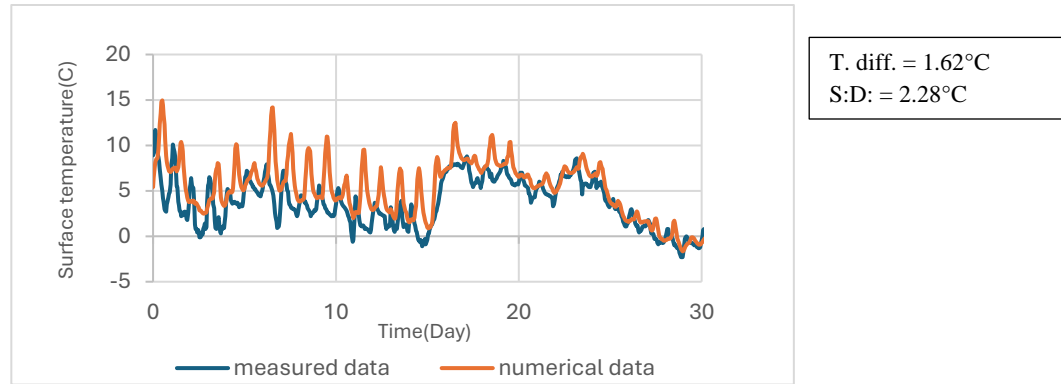


Figure 15: Mean difference and standard deviation of the road surface temperature(degC) between the numerical simulation model and the measured data for the test site E18

The surface temperature based on the Hydronic Heating Pavement model without embedded pipes is shown in Figure 16. When no heating pipes are installed underground, the road surface temperature ranges from -16.24 C to 38.4 C.

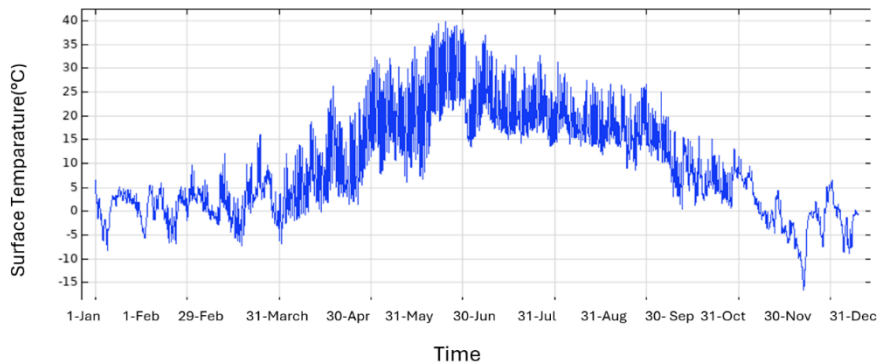


Figure 16: Numerical calculated surface temperature using the climate data of test site E18 for the case of without pipe

The results were obtained for the E18 test site using two different approaches: one based on measured data from the site and the other on numerically calculated values. The analysis reveals that the maximum number of hours with the surface temperature below 0°C was 2121 hours for the measured data and 1638 hours for the numerically calculated data for the year 2023.

The calculated surface temperature was used to determine the number of hours with slippery conditions on the road surface, based on the slippery condition equation. The cumulative frequency of slippery conditions versus ambient temperature is shown in Figure 17. It can be observed that 60% of slippery conditions occur when the ambient air temperature is below 0°C. Additionally, for 5% of the year. Slippery conditions occur when the air temperature is below -10°C. It is important to note that slippery conditions do not occur on the road surface when the air temperature is above 4°C.

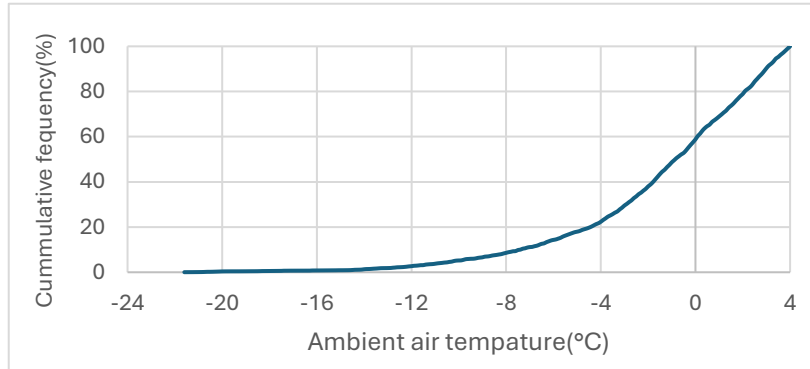


Figure 17: Cumulative frequency of the road surface versus ambient air temperature using test site E18 climate data

## 5.2 Numerical modelling of Gothenburg site

This section presents the required energy for anti-icing the roads and the number of hours with slippery conditions. Numerical simulation was performed with heating pipes embedded in the pedestrian path using the implicit time-stepping method. The time-step was 1hour based on the data provided by a researcher from Trafikverket and SMHI. The reference model was selected to run the initial simulation and the data used for the simulation are presented in Table 7.

Table 7: Information about the initial simulated HHP system in this study(Mirzananamadi, Hagentoft, & Johansson, 2018)

S. NO	Parameter	Value	Unit
1	Thermal conductivity of pipe material	0.42	W/ (m.K)
2	Density of pipe material	1100	kg/m <sup>3</sup>
3	Specific heat capacity of pipe material	1465	J/ (kg. K)
4	Outer diameter of the embedded pipes	25	mm
5	Pipe thickness	2.3	mm
6	Fluid temperature (when it is running)	10	°C
7	Distance between the pipes	100	mm
8	Embedded depth (from center of the pipe to the surface)	50	mm
9	Emissivity of the road surface	0.9	----
10	Absorptivity of the road surface	0.6	---

The surface temperature based on the Hydronic heating pavement model with embedded pipes is shown in Figure 18. When heating pipes are installed underground, the road surface temperature ranges from  $-2.66^{\circ}\text{C}$  to  $37.2^{\circ}\text{C}$ . These results were obtained for the Gothenburg test site using numerically calculated data. The analysis reveals that the maximum number of hours with the surface temperature below  $0^{\circ}\text{C}$  was 922 hours for the year 2021, 2022 and 2023.

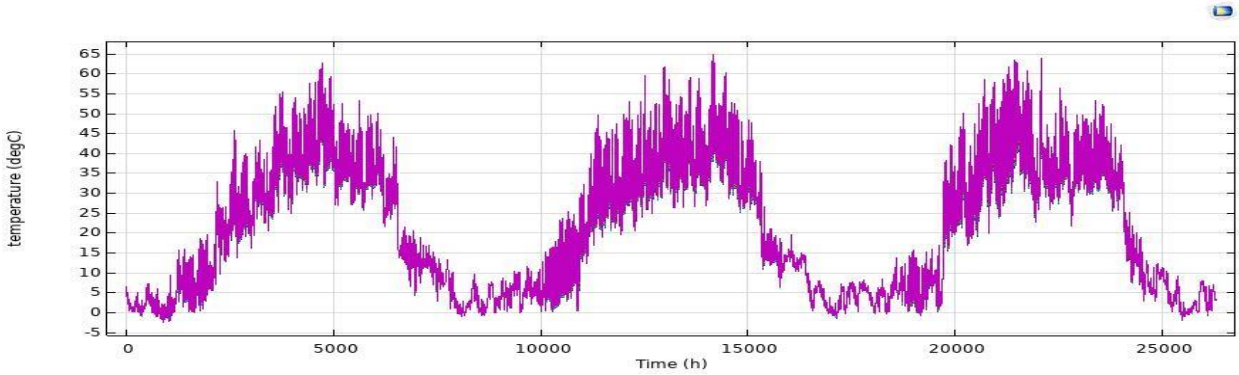


Figure 18: Numerical calculated surface temperature using the climate data of Gothenburg for the case with heating pipe

The calculated surface temperature was also used to estimate the number of hours of slippery conditions on the road, using the slippery conditions equations. The accumulative frequency of slippery conditions versus ambient temperature is illustrated in Figure 19. It can be observed that 40% of slippery conditions occur when the ambient air temperature is below  $0^{\circ}\text{C}$  and 7.4% of the year experiences slippery conditions when the temperature drops below  $-6^{\circ}\text{C}$ . Notably slippery conditions do not occur on the road surface when the air temperature exceeds  $4^{\circ}\text{C}$ .

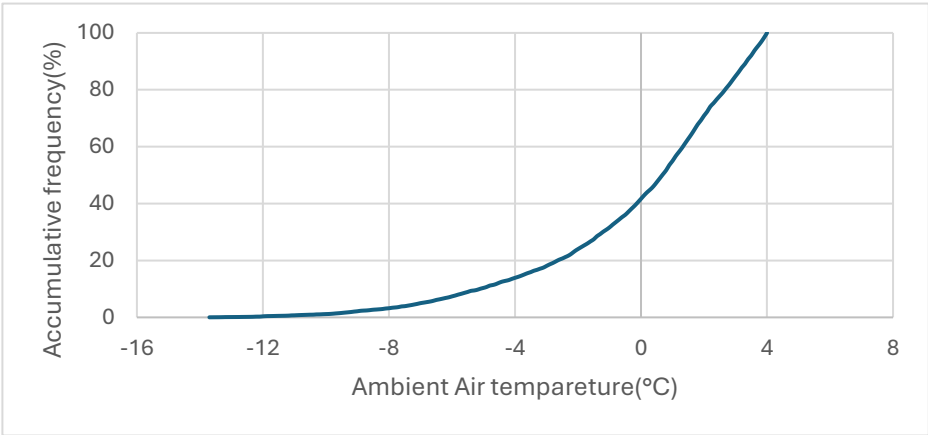


Figure 19: Cumulative frequency of the road surface versus ambient air temperature using Gothenburg site data

### 5.2.1 The required energy for anti-icing and slippery conditions of road surface

From the simulated model, the surface temperature results were obtained, and the heat flow was calculated. The total annual energy required was determined by using the relevant equation  $E_r$ , yielding 62.97 kWh per year. The mean heat flow from a single pipe when the system was active is 481.3 w/m. According to (Mirzanimadi, 2017) the required heat flow for snow melting typically ranges from 44 Kwh to 1600kwh, additionally the number of slippery condition hours decreased by a factor of five, down to 307 hours. The slippery conditions and the anti-icing effectiveness were based solely on surface heating, with factors such as snow weight, heat from vehicular movement and friction being neglected. Table 8 summarizes the number of hours with slippery conditions in the numerical model using the HHP system as well as the annual energy required.

Table 8: Required energy for anti-icing the road surface and mean heat flow from a single pipe of the HHP system

Annual required energy for anti-icing the road surface, $E_r$ (kWh/ (m <sup>2</sup> . year))	Mean heat flow from a single pipe $q_{\text{pipe-heating}}$ (W/m <sup>2</sup> ) when the system is on
62.97	481.3

Table 9 and Table 10 represent the estimated number of hours with slippery conditions on the road surface, both with and without heating systems. For the case without a heating system, the test site E18 had two different values: one based on measured data and the other from the numerically simulated model. The measured data showed 1937 hours of slippery conditions, while the numerical model predicted 1492 hours. With the heating applied to the road surface, the number of slippery hours was further reduced to 307 hours per year

Table 9: Slippery condition of road surface without heating pipes

Without considering heating system	
Numerical	1492/ year
Measured	1937/ year

Table 10: Slippery condition of road surface with heating pipes

Heating the road surface using the HHP system		
	For 3 years	For 1 year
Numerical	922	307

## 5.3 Sensitivity Analysis for different parameters

This section presents the results from the numerical simulation of HHP model. All other parameters were kept constant while a sensitivity analysis was conducted on various factors such as: thermal conductivity, distance between pipes, fluid temperature, absorptivity and embedded depth of the pipes. The analysis was based on the assumptions made by varying one parameter from Table 7 while all others remained unchanged.

### 5.3.1 Thermal conductivity of wearing layer

From the literature (Mirzanimadi, Hagentoft, Johansson, et al., 2018) the thermal conductivity of asphalt concrete ranges from 0.7 to 2.9 W. In this section, three different thermal conductivity of the wearing layer are considered that are 1 W/m. K, 2 W/m. K and 3 W/m. K to analyze the effects on the anti-icing performance of the HHP system. Density and the specific heat capacity of the wearing layer are assumed to be constant at 2415 and 848, respectively. These values were related to the asphalt concrete of ABT8. The annual required energy and the remaining hours of the slippery conditions on the pedestrian surface are shown in the Figure 20

Further by increasing the thermal conductivity of the wearing layer from 1 to 3W/m. K, the annual required energy increases from 56.7 to 66.66kWh/ (m<sup>2</sup>. year). The number of slippery condition hours decreases from 1076 hours to 907 hours for the respective thermal conductivity value.

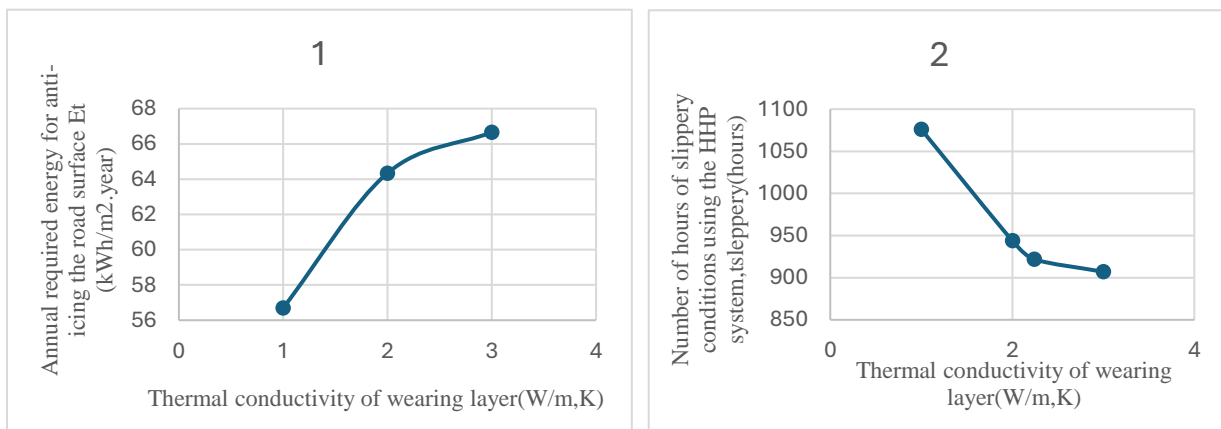


Figure 20: The effect of the thermal conductivity of wearing layer on the anti-icing performance of the HHP system using GBG data (1) The annual required energy for anti-icing (2) slippery condition on the road surface

### 5.3.2 Distance between the pipes

To analyze the effects of distance between the pipes on the anti-icing performance of HHP system, four different distances (center to center) of 100 mm, 200 mm, 300 mm and 400 mm were considered. The minimum distance between the pipes was four times the outer diameter of the pipe. Moreover, based on (Mirzanimadi, Hagentoft, Johansson, et al., 2018) the maximum distance between the two pipes was taken to be 400mm. The annual required energy and the remaining hours of the slippery conditions on the pedestrian surface are shown in the Figure 21

While increasing the pipe distances from 100mm to 400mm, the annual required energy decreases from 62.9 kWh/ (m<sup>2</sup>. year) to 22.29 kWh/ (m<sup>2</sup>. year) and slippery conditions increase from 922hours for three years to 1743 hours for three years.

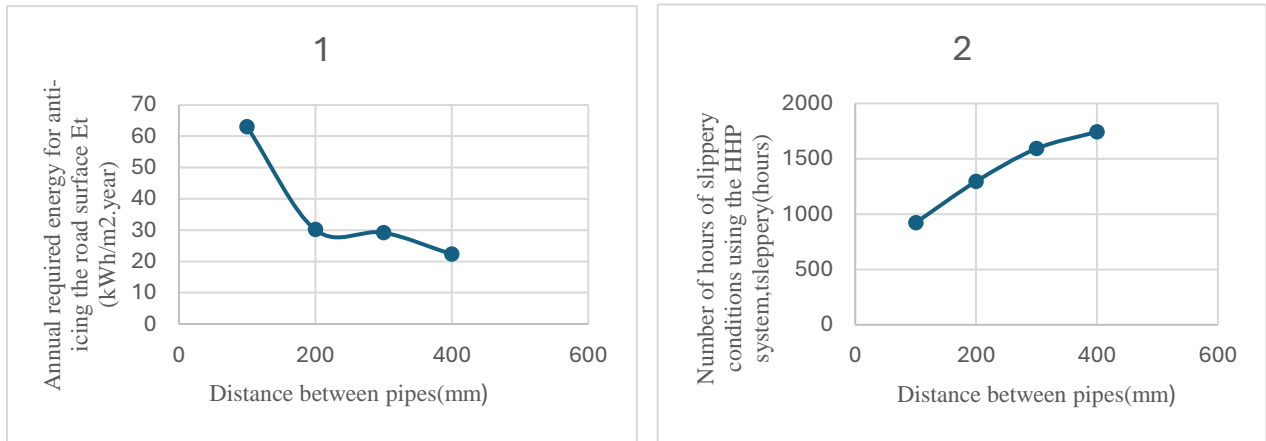


Figure 21: The effect of distance between the pipe on the anti-icing performance of the HHP system using GBG data (1)The annual required energy for anti-icing (2)slippery condition on the road surface

### 5.3.3 Fluid temperature

The effect of the fluid temperature on the anti-icing performance of the HHP system is presented below. As per (Mirzananadi, Hagentoft, Johansson, et al., 2018) the recommended fluid temperature for HHP ranges to be 5 °C to 20 °C which has been considered in this analysis. The annual required energy varies from 41.8 kWh/ (m<sup>2</sup>. year) to 92.8 kWh/ (m<sup>2</sup>. year) for the fluid temperature values of 5, 10, 15 and 20 °C. The annual required energy and the remaining hours of the slippery conditions on the pedestrian surface are shown in the Figure 22

Based on the analysis the slippery condition of the road decreases while the fluid temperature increases, making it less risky for the slippery condition of the surface of the road. The number of hours of slippery conditions varies from 1386 hours for 3year to 316hours for 3year with respect to the fluid temperatures ranging from 5°C to 20°C.

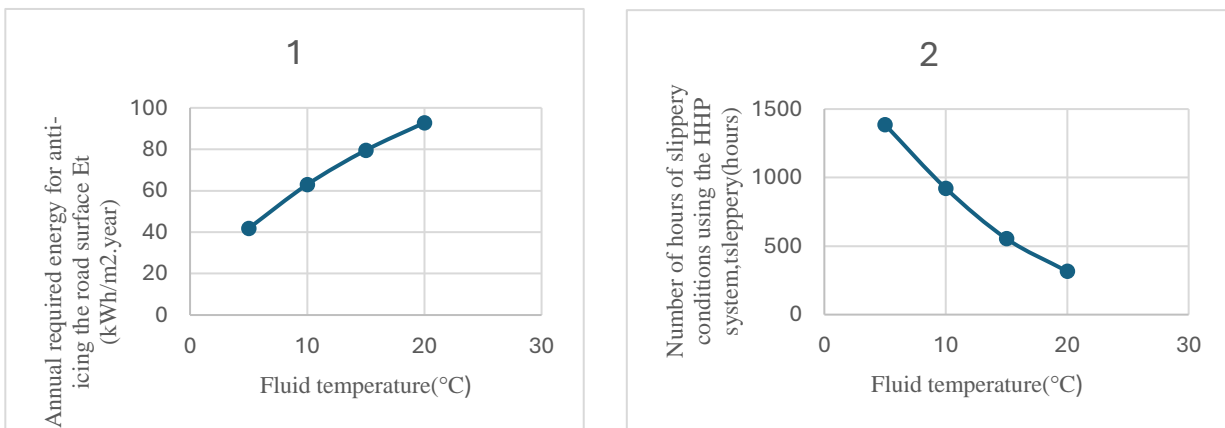


Figure 22: The effect of different Fluid temperatures on the anti-icing performance of the HHP system using GBG data (1)The annual required energy for anti-icing(2)slippery condition on the road surface

### 5.3.4 Absorptivity of the road surface

The absorptivity ranges from 0.6 to 0.95 based on (Mirzanimadi, Hagentoft, Johansson, et al., 2018). The variation of annual energy requirement to different absorptivity and slippery condition values are shown in Figure 23. Five different absorptivity values of 0.6, 0.7, 0.8, 0.9 and 0.95 are considered for the analysis. Higher absorptivity on the road surface requires more solar radiation, resulting in increased temperature of the road surface and lowering the risk of slippery conditions. The annual required energy and the remaining hours of the slippery conditions on the pedestrian surface are shown in the Figure 23.

The annual energy requirement decreases from 62.92kWh/ (m<sup>2</sup>. year) to 57.88 kWh/ (m<sup>2</sup>. year) by increasing the absorptivity values from 0.6 to 0.95. The slippery condition of the pedestrian path decreases from 922hours for 3years to 833 hours for 3 years.

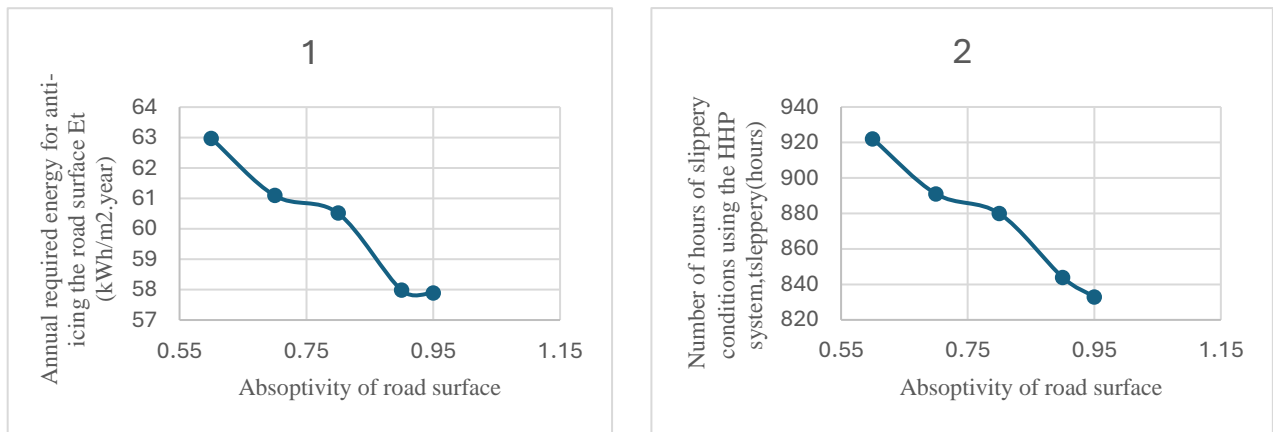


Figure 23: The effect of Absorptivity of the road surface on the anti-icing performance of the HHP system using GBG data(1)The annual required energy for anti-icing(2)slippery condition on the road surface

### 5.3.5 Embedded depth of pipe

Based on (Mirzanimadi, Hagentoft, Johansson, et al., 2018) shallower embedded pipes are exposed to higher risk of damage under traffic loads. The recommended embedded depth should be deeper than 50mm. Since the analysis is for pedestrian path the risk of load under traffic is neglected resulting in placing the pipes at a near shallower depth of 25mm. here four different embedded depths of 25mm,50mm,75mm and 100mm are analyzed. The annual required energy decreases from 86.8 to 42.2 as the embedded depth increases as shown in Figure 24.

The number of hours for the slippery condition increases from 640 hours for 3 years to 1213 hours for 3 years when the depth of the pipe increases.

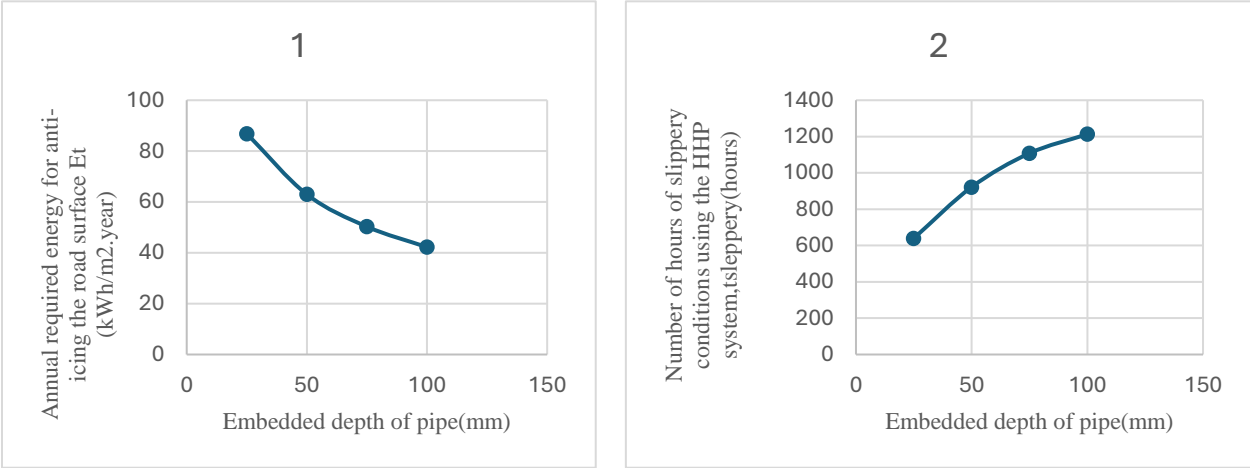


Figure 24: The effect of embedded depth of the pipe on the anti-icing performance of the HHP system using GBG data (1)The annual required energy for anti-icing(2)slippery condition on the road surface

## 6. Summary and Conclusion

This study aimed to investigate the feasibility of utilizing the Hydronic Heating Pavement (HHP) system for solar energy collection and anti-icing on pedestrian roads. The Objective was to analyse how different design options of HHP systems affect anti-icing performance using a numerical simulation model. The study began with the assumption that there was no existing snow or friction caused by movement on pedestrian road and the slippery conditions occur only when moisture on the road surface turns to liquid. The heating system was activated only when the surface temperature fell below 0°C and the dew point temperature, preventing water vapor from condensing into liquid and forming ice on the surface.

Two different numerical models of the Hydronic Heating Pavement (HHP) systems were developed using COMSOL Multiphysics 6.2. The models were based on two different test sites: Test site E18 in Östersund and a locally situated site Gothenburg. These numerical models were simulated for two different scenarios, with Test site E18 used to evaluate the model without any heating system beneath the motorway. The validation results showed a mean temperature difference of 0.77°C between the surface temperature obtained from the numerical model and the measured data, with a standard deviation of 5.43°C. Additionally, the Gothenburg site was simulated using a 2D numerical model to analyze the surface temperature and develop a pedestrian pathway with an embedded heating system. The results indicate that heating the road surface using the HHP system reduced the number of hours of slippery condition to 332 h, compared to 2121 h for the test site E18 without a heating system.

By using a reference model with fixed values for different parameters of pedestrian pathways, results were obtained from the numerical model, showing an annual required energy of 62.4 kWh/m<sup>2</sup> per year for anti-icing the road surface and a mean heat flow of 481.3 W/m<sup>2</sup> per year from a single pipe in the HHP system. Furthermore, a sensitivity analysis was conducted to evaluate various parameters affecting the energy of the HHP systems, such as: a) thermal conductivity of the wearing layer, b) distance between the pipes, c) fluid temperature inside the pipe, d) absorptivity on the road surface, and e) the embedded depth of pipes.

The results from the sensitivity analysis showed the following:

- Increasing the thermal conductivity of the asphalt layer reduces the number of hours of slippery conditions by nearly 10%.
- The distance between pipes is a critical factor; by increasing the distance between the pipes, the number of hours increases by more than double for the slippery conditions.
- Raising the fluid temperature, although required more than twice the annual energy supply, reduces the number of hours of slippery conditions by more than four times.
- Increasing the absorptivity of the road surface results in a warmer surface, which decreases the number of hours of slippery conditions by almost 10%.

- Shallower pipe placement is nearly halving the number of hours of slippery conditions.

In this study, it is acknowledged that changing the specific heat capacity could influence the results. However, due to the time constraints, this factor was not investigated. The same applies to other parameters that could have been used for sensitivity analysis. While this research utilized parameters based on existing literature relevant to the study, it is important to note that additional parameters could have been considered. The limitations in time, budget and in some cases, knowledge prevented a more detailed analysis.

The study further discusses the main difference between roads and pedestrian pathways that affect the energy required for anti-icing using the Hydronic Heating Pavement system.

- Road lanes are typically around 3.5m wide, while pedestrian pathways are much narrower, approximately 0.5m. This results in around 7 times less energy being required to heat pedestrian pathways compared to motorways, even if the pipe distance and depth remain the same
- Roads are designed to withstand heavy vehicular loads, while pedestrian pathways do not experience the same load
- With the same pipe distance and depth used for both roads and pedestrian pathways, the narrower width of pedestrian pathways allows for more efficient heating as less energy is required, which helps the HHP system to be optimized for small areas, potentially reducing the number of pipes.

Based on the energy required per year for the Gothenburg site, it is observed that the annual energy demand is approximately 62.57 kWh/m<sup>2</sup> per year. In comparison, the total solar irradiation collected for Gothenburg is around 1022.725 kWh/m<sup>2</sup> per year. According to the literature (Mirzanimadi, 2019) solar energy could be harvested by about 30% for a year, further in this study harvesting about 30% of this available solar energy, it yields 306.875 kWh/m<sup>2</sup> per year. This amount is five times the required energy, making it more than sufficient to run the HHP system. This highlights the solar energy is a highly reliable and sustainable renewable energy source for running the system effectively.

# 7. Future work

While this thesis has aimed to cover a significant portion of study, further research is required in several areas, the future work could focus on:

- Evaluating the thermal properties of road materials such as specific heat capacity could give a better insight into the hydronic heating pavement
- Investigating the type of fluid used within the pipes
- Exploring different materials or alternatives for heating pipes to improve durability and better performance
- Further analysis of materials used in the pavement layers, as different asphalt compositions may impact heat conductivity.

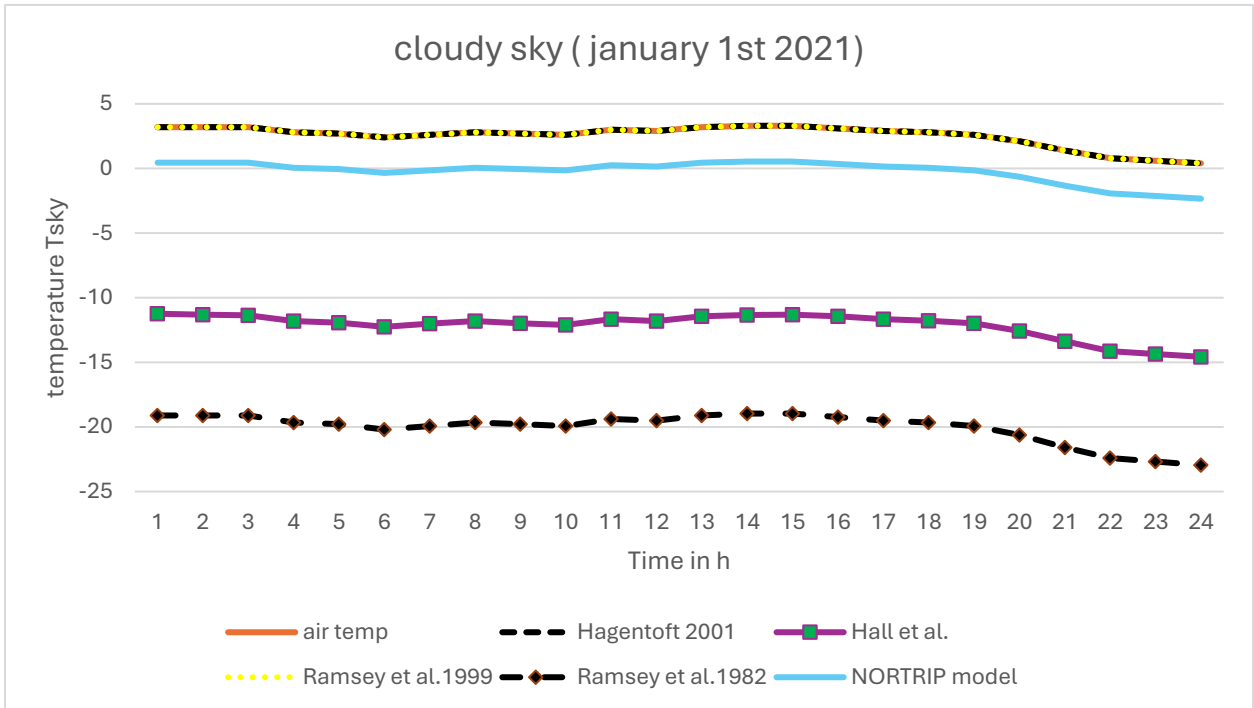
# Reference

- Andersson, A. K. (2010). *Winter road conditions and traffic accidents in Sweden and UK : present and future climate scenarios [Elektronisk resurs]*. Dept. of Earth Sciences, Physical Geography, University of Gothenburg.
- Bärwolff, M., Reinartz, A., & Gerike, R. (2021a). Correlates of Pedestrian and Cyclist Falls in Snowy and Icy Conditions. *Transactions on Transport Sciences*, 12(3), 67–77. <https://doi.org/10.5507/tots.2021.007>
- Bärwolff, M., Reinartz, A., & Gerike, R. (2021b). Correlates of Pedestrian and Cyclist Falls in Snowy and Icy Conditions. *Transactions on Transport Sciences*, 12(3), 67–77. <https://doi.org/10.5507/tots.2021.007>
- Eriksson, J., Henriksson, P., & Rizzi, M. (n.d.). *Oskyddade trafikanters inblandning i olyckor och deras skadeutfall*.
- Fossum, M., & Ryeng, E. O. (2022). Pedestrians' and bicyclists' route choice during winter conditions. *Urban, Planning and Transport Research*, 10(1), 38–57. <https://doi.org/10.1080/21650020.2022.2034524>
- Gitelman, V., Balasha, D., Carmel, R., Hendel, L., & Pesahov, F. (2012). Characterization of pedestrian accidents and an examination of infrastructure measures to improve pedestrian safety in Israel. *Accident Analysis and Prevention*, 44(1), 63–73. <https://doi.org/10.1016/j.aap.2010.11.017>
- Glagolev, S., Shevtsova, A., & Shekhovtsova, S. (2018). Basis for application of new-generation anti-icing materials as an efficient way to reduce the accident rate on roads in winter. *Transportation Research Procedia*, 36, 193–198. <https://doi.org/10.1016/j.trpro.2018.12.063>
- Hippi, M., Kangas, M., Ruuhela, R., Ruotsalainen, J., & Hartonen, S. (2020). RoadSurf-Pedestrian: a sidewalk condition model to predict risk for wintertime slipping injuries. *Meteorological Applications*, 27(5). <https://doi.org/10.1002/met.1955>
- Hossain, S. M. K., Olesen, A. J., & Fu, L. (2014a). Effectiveness of anti-icing operations for snow and ice control of parking lots and sidewalks. *Canadian Journal of Civil Engineering*, 41(6), 523–530. <https://doi.org/10.1139/cjce-2013-0587>
- Hossain, S. M. K., Olesen, A. J., & Fu, L. (2014b). Effectiveness of anti-icing operations for snow and ice control of parking lots and sidewalks. *Canadian Journal of Civil Engineering*, 41(6), 523–530. <https://doi.org/10.1139/cjce-2013-0587>
- Juga, I., & Vajda, A. (2012). *ID: 0042 The effect of weather on transportation: Assessing the impact thresholds for adverse weather phenomena*.

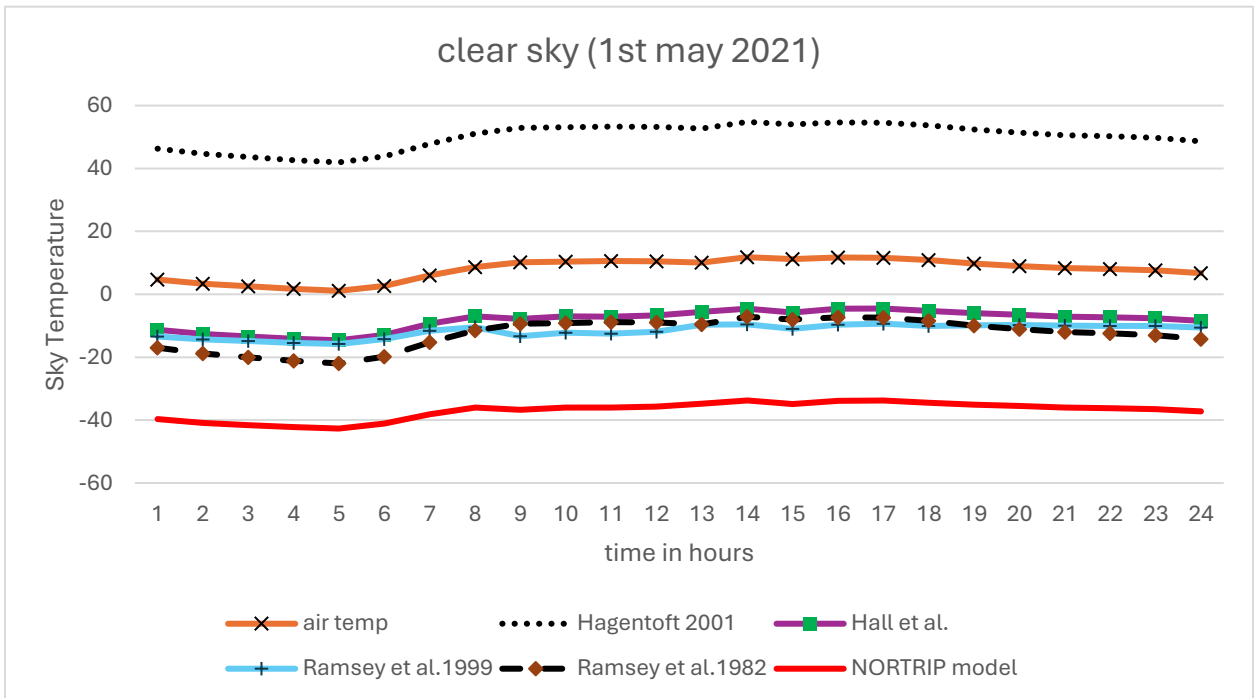
- Levulyte, L. (2017). PEDESTRIANS' ROLE IN ROAD ACCIDENTS. *INTERNATIONAL JOURNAL FOR TRAFFIC AND TRANSPORT ENGINEERING*, 7(3). [https://doi.org/10.7708/ijtte.2017.7\(3\).04](https://doi.org/10.7708/ijtte.2017.7(3).04)
- Liang, S., Leng, H., Yuan, Q., Wang, B. W., & Yuan, C. (2020a). How does weather and climate affect pedestrian walking speed during cool and cold seasons in severely cold areas? *Building and Environment*, 175. <https://doi.org/10.1016/j.buildenv.2020.106811>
- Liang, S., Leng, H., Yuan, Q., Wang, B. W., & Yuan, C. (2020b). How does weather and climate affect pedestrian walking speed during cool and cold seasons in severely cold areas? *Building and Environment*, 175. <https://doi.org/10.1016/j.buildenv.2020.106811>
- Michelle Akin, by, Jiang Huang, P., Shi, X., David Veneziano, P., & Williams, D. (2013). *Snow Removal at Extreme Temperatures Final Report*.
- Mirzanamadi, R. (2017). *Ice free roads using hydronic heating pavement with low temperature Thermal properties of asphalt concretes and numerical simulations*.
- Mirzanamadi, R., Hagentoft, C. E., & Johansson, P. (2018). An analysis of hydronic heating pavement to optimize the required energy for anti-icing. *Applied Thermal Engineering*, 144, 278–290. <https://doi.org/10.1016/j.applthermaleng.2018.08.053>
- Mirzanamadi, R., Hagentoft, C. E., & Johansson, P. (2020). Coupling a Hydronic Heating Pavement to a Horizontal Ground Heat Exchanger for harvesting solar energy and heating road surfaces. *Renewable Energy*, 147, 447–463. <https://doi.org/10.1016/j.renene.2019.08.107>
- Mirzanamadi, R., Hagentoft, C. E., Johansson, P., & Johansson, J. (2018). Anti-icing of road surfaces using Hydronic Heating Pavement with low temperature. *Cold Regions Science and Technology*, 145, 106–118. <https://doi.org/10.1016/j.coldregions.2017.10.006>
- Mirzanamadi, R., Johansson, P., & Grammatikos, S. A. (2018). Thermal properties of asphalt concrete: A numerical and experimental study. *Construction and Building Materials*, 158, 774–785. <https://doi.org/10.1016/j.conbuildmat.2017.10.068>
- Mirzanamadi, Raheb. (2019). *Utilizing solar energy for anti-icing road surfaces using hydronic heating pavement with low temperature*. Department of Architecture and Civil Engineering, Chalmers University of Technology.
- Narváez, Y. V., Parra Sierra, V., Peña Cárdenas, F., Ruíz Ramos, L., Zamorano González, B., Vargas Martínez, J. I., & Monreal Aranda, O. (2019). Road risk behaviors: Pedestrian experiences. *Traffic Injury Prevention*, 20(3), 303–307. <https://doi.org/10.1080/15389588.2019.1573318>
- SMHI. . (n.d.).

- Sollén, S., & Casselgren, J. (2021). Large-scale implementation of floating car data monitoring road friction. *IET Intelligent Transport Systems*, 15(6), 727–739. <https://doi.org/10.1049/itr2.12039>
- Svelander, S., & Turefeldt, M. (n.d.). *Effekterna av termiska egenskaper hos asfaltmaterial på temperaturförändringen The effects of thermal properties of asphalt materials on the temperature change Examensarbete inom högskoleingenjörsprogrammet samhällsbyggnadsteknik*. [www.chalmers.se](http://www.chalmers.se)
- Xu, H., Wang, D., Tan, Y., Zhou, J., & Oeser, M. (2018). Investigation of design alternatives for hydronic snow melting pavement systems in China. *Journal of Cleaner Production*, 170, 1413–1422. <https://doi.org/10.1016/j.jclepro.2017.09.262>
- Yu, W., Chen, L., Yi, X., & Guo, M. (2014). *State of the art and practice of pavement anti-icing and de-icing techniques Sciences in Cold and Arid Regions State of the art and practice of pavement anti-icing and de-icing techniques*. <https://doi.org/10.3724/SP.J.1226.2014.00014>

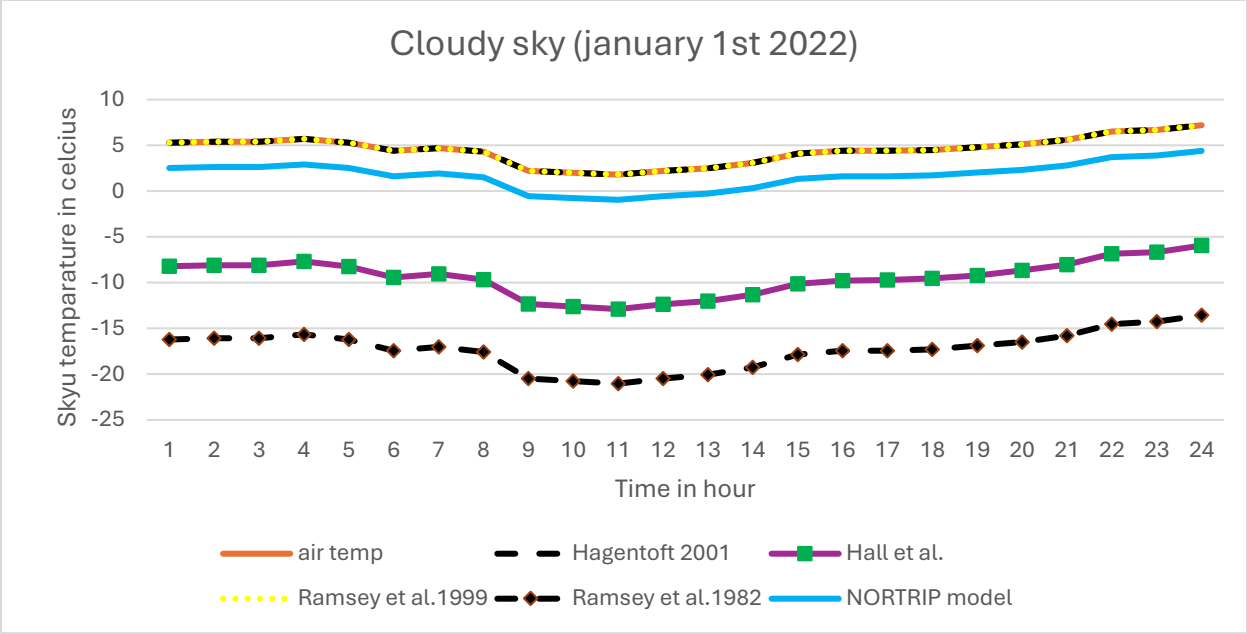
# Appendix



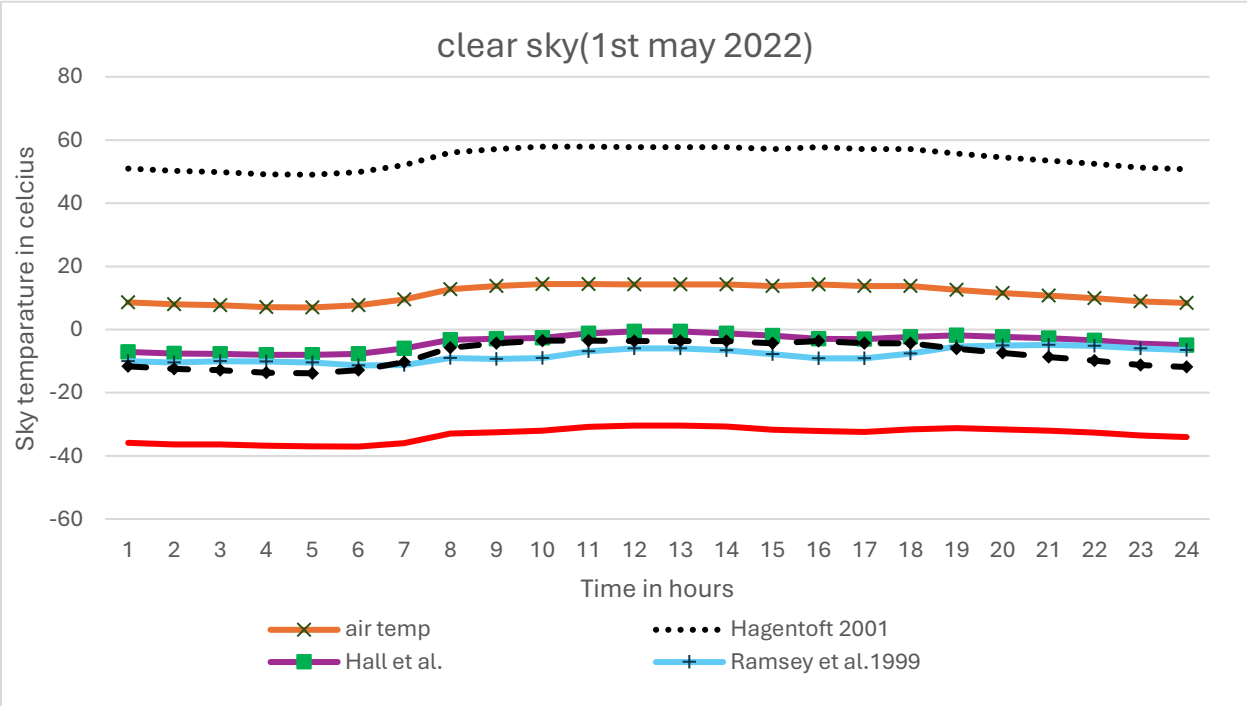
Scatter plot of Sky temperature for different models for cloudy sky year 2021



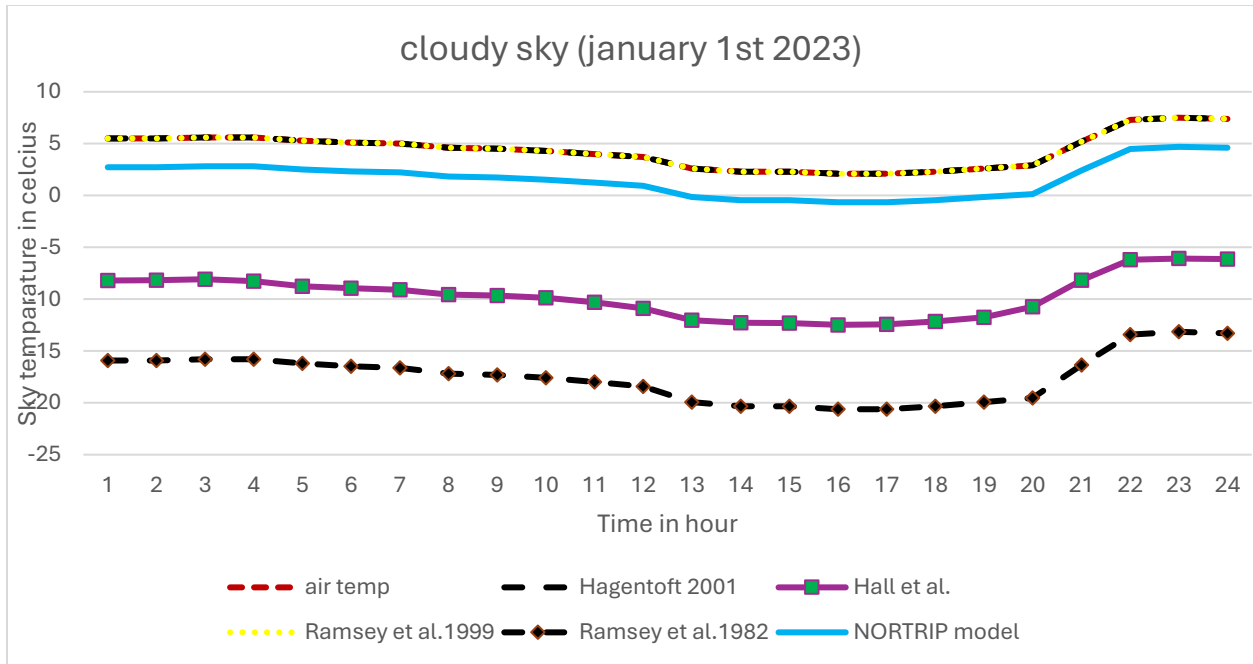
Scatter plot of Sky temperature for different models for clear sky year 2021



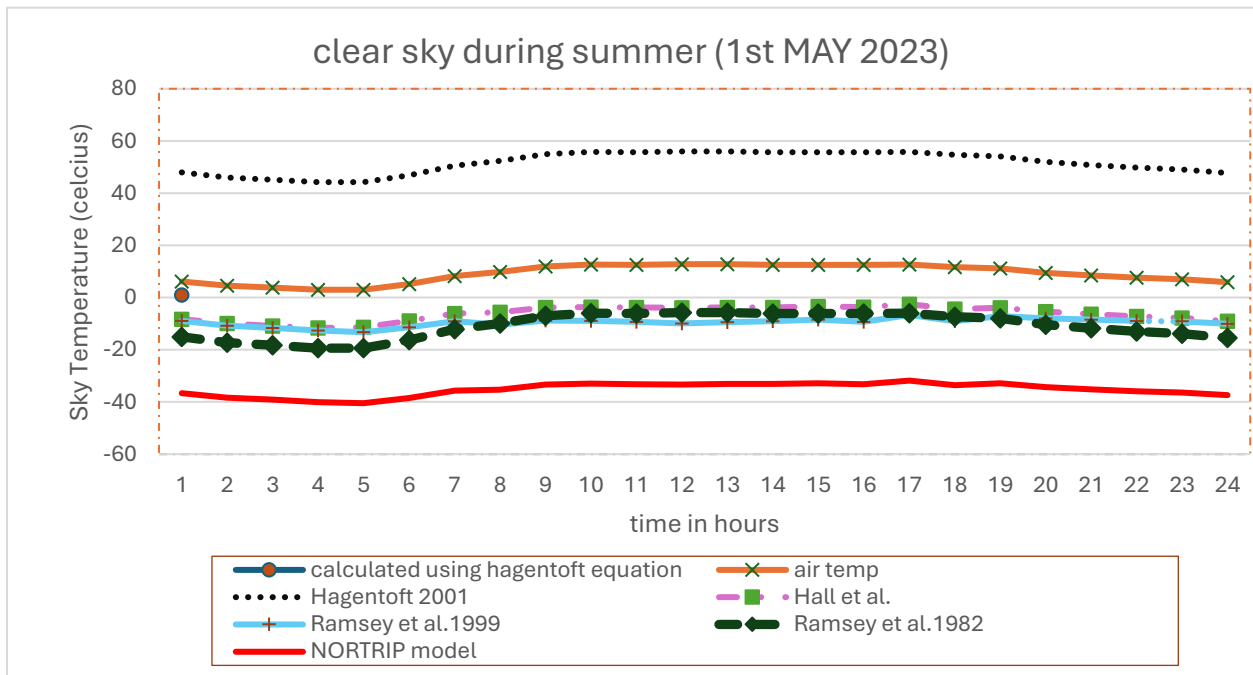
Scatter plot of Sky temperature for different models for cloudy sky year 2022



Scatter plot of Sky temperature for different models for clear sky year 2022



Scatter plot of Sky temperature for different models for cloudy sky year 2023



Scatter plot of Sky temperature for different models for clear sky year 2023



**CHALMERS**  
UNIVERSITY OF TECHNOLOGY